electronics

MDPI

Article

Ring-Shaped Wheeled Mobile Robot Circulation with Modified Van der Pol Limit-Cycle Reference

Jesus Quiros [1], Luis T. Aguilar [1,*], Ulises Orozco-Rosas [2] and Victor Manuel Juárez-Luna [3]

[1] Centro de Investigacion y Desarrollo de Tecnologia Digital, Instituto Politécnico Nacional, Tijuana 22435, Mexico; jquiros@citedi.mx
[2] CETYS Universidad, Av. CETYS Universidad No. 4, Fracc. El Lago, Tijuana 22210, Mexico; ulises.orozco@cetys.mx
[3] Facultad de Ingeniería, Arquitectura y Diseño, Universidad Autónoma de Baja California, Ensenada 22860, Mexico; juarezv@uabc.edu.mx
* Correspondence: laguilarb@ipn.mx; Tel.: +52-(664)-370-8232

Abstract

Defining and tracking trajectories in complex environments for nonholonomic mobile robots are challenging due to the underactuated dynamics and nonintegrable velocity constraints of these robots, which preclude smooth, time-invariant feedback stabilization and yield uncontrollable linearizations around equilibrium points. As a result, maintaining structured motions such as ring-shaped limit cycles becomes particularly difficult under large initial deviations or external disturbances. In this paper, a control framework based on a dynamically generated reference trajectory is proposed, where the desired motion is defined by a modified Van der Pol oscillator. Unlike conventional approaches relying on predefined geometric paths, the proposed method embeds the target orbit into a dynamic auxiliary nonlinear system whose trajectories converge to a stable limit cycle, enabling local asymptotic convergence to the desired motion. A discontinuous robust control law is designed for a perturbed wheeled mobile robot, and the resulting closed-loop system is analyzed within the framework of solutions of systems with discontinuous right-hand sides. It is shown that the tracking error dynamics are uniformly and ultimately bounded with respect to matched disturbances and that, in the disturbance-free case, the tracking errors converge asymptotically to the origin. As a consequence, the robot's trajectory converges to the invariant limit cycle of the reference dynamics, therebydriving the robot's trajectory toward the invariant limit cycle of the reference dynamics. The simulation results demonstrate an improvement in the transient response relative to standard circular reference tracking. The experimental results further corroborate these findings, showing that the modified Van der Pol reference keeps the position tracking errors tightly bounded, while mitigating the large initial overshoot associated with the circular reference.

Keywords: wheeled mobile robot; path tracking; Van der Pol oscillator; vehicle flow; sliding modes

Academic Editor: Nikolay Hinov

Received: 4 May 2026
Revised: 22 May 2026
Accepted: 27 May 2026
Published: 4 June 2026

1. Introduction

Motivation: Standard trajectory tracking approaches for wheeled mobile robots rely on predefined geometric paths (e.g., circles or splines), which often lead to large transient errors and abrupt control actions when the robot is initialized far from the path. This limitation is particularly critical in applications such as roundabout navigation, where smooth entry into circulating flow is essential for safety and comfort [1,2].

In contrast to geometric path-following methods, dynamic-system-based trajectory generation offers an alternative paradigm in which the desired motion emerges from the evolution of an autonomous system [3,4]. In this context, the problem of circular navigation can be naturally interpreted as convergence toward a closed orbit. This perspective motivates the use of nonlinear oscillators with a stable limit cycle that attracts trajectories from a neighborhood of the orbit to generate reference motions.

The Van der Pol equation [5] is a nonlinear oscillator originally introduced to model electrical circuits with nonlinear damping [6]. It exhibits self-sustained oscillations and admits a stable limit cycle. It has also been used to generate rhythmic patterns in legged robot locomotion [7,8], large force generation and a control method for a manipulator that exploits its oscillatory motion [9], to model biological rhythms [10], and to design trajectory generators for wheeled mobile robots [11].

The classical Van der Pol equation generates periodic solutions whose geometry depends implicitly on system parameters. To address this limitation, a modified version of the Van der Pol equation was introduced in [12], where nonlinear damping depends on both the state and its derivative. This formulation allows the limit cycle to be explicitly shaped in the phase plane, rather than being implicitly determined by system parameters. Such a construction has proven useful in applications ranging from underactuated mechanical systems [13] to infinite-dimensional settings [14].

In this paper, we propose a control framework for wheeled mobile robots based on a modified Van der Pol oscillator used as a dynamic reference generator. Unlike geometric path descriptions, the proposed approach generates the reference trajectory through an auxiliary dynamical system whose limit cycle defines the desired orbit. As a result, the reference trajectory evolves smoothly and induces a spiraling transient behavior that guides the robot toward the desired orbit.

Unlike conventional geometric path-following formulations, the proposed approach does not enforce the orbit directly through the controller or through constraints embedded into the robot's dynamics. Instead, the desired motion emerges from the attractivity properties of a dynamic auxiliary nonlinear system that is structurally independent of the vehicle model. Consequently, the orbital stabilization problem is reformulated as the robust tracking of an externally generated attracting invariant set. This separation between orbit generation and vehicle stabilization constitutes a key conceptual distinction from prior oscillator-based navigation approaches. Moreover, it allows the transient geometry of the reference trajectory to evolve continuously before convergence to the final orbit.

Accordingly, the problem is formulated as the asymptotic tracking of a dynamically generated reference trajectory whose internal dynamics converge to a stable limit cycle. To this end, we design a robust control law for a perturbed nonholonomic robot model and analyze the resulting closed-loop system using Lyapunov techniques. The presence of discontinuities in the control input is addressed within the framework of Filippov solutions.

Contribution: The main contributions of this work can be summarized as follows:

- The modified Van der Pol oscillator admits two invariant sets: an unstable equilibrium at the origin and a locally asymptotically stable limit cycle, which defines the desired orbit.
- The control objective is formulated as the asymptotic tracking of a dynamically generated reference trajectory converging to an invariant limit cycle.
- The proposed framework enables bidirectional circulation along the same invariant orbit without modifying the underlying oscillator dynamics, allowing the direction of traversal to be adjusted independently through the orientation reference, while preserving both the geometric path and its intrinsic attractivity. Moreover, this feature allows the seamless adaptation to different traffic conventions (e.g., clockwise

or counterclockwise roundabout navigation) without requiring the redesign of the reference generator.

- A robust control law is designed for a perturbed nonholonomic robot, and the resulting closed-loop system is shown to be well-posed in the Filippov sense. The proposed controller attenuates the effect of matched disturbances and modeling uncertainties, while, in the disturbance-free case, convergence toward the desired orbit is established via an invariance principle for discontinuous systems [15].

In particular, in contrast to purely geometric circular references, the proposed approach provides a continuous mechanism for guiding the robot toward the orbit, reducing large initial deviations and avoiding abrupt control actions.

Additionally, the modified Van der Pol system serves as a dynamic trajectory planner that continuously reshapes the transient response before convergence to the final orbit. Consequently, unlike predefined geometric circular references, the proposed approach guides the robot through the attractivity properties of an autonomous nonlinear flow. The observed reduction in overshoot therefore originates primarily from the transient deformation induced by the auxiliary dynamics rather than from the sliding-mode structure itself, whose role is limited to robustness against matched disturbances and modeling uncertainties.

Compared with the blimp-based approach in [11], where convergence to the Van der Pol oscillation is enforced through constraint embedding and state-dependent linearization, the present work employs modified Van der Pol dynamics as an external autonomous reference generator that remains structurally independent of the robot model. The resulting framework formulates the problem as the robust tracking of a dynamically generated attracting limit cycle with particular motivation toward smooth transient entry into circulating traffic flows in autonomous roundabout navigation.

This paper is organized as follows: Section 2 introduces the robot model and formalizes the control objective. Section 3 presents the construction of the Van der Pol-based reference trajectories. Section 4 develops the control law and provides the stability analysis. Section 5 illustrates the effectiveness of the proposed approach through simulation results. Section 6 includes experiments conducted on a small-scale wheeled mobile robot. Finally, Section 7 concludes this paper and outlines future research directions.

2. Dynamic Model and Problem Statement

To describe the motion of a wheeled mobile robot (WMR), let us consider the following perturbed kinematic model:

$$\dot{x} = (v + d_1)\cos(\theta) \tag{1}$$

$$\dot{y} = (v + d_1)\sin(\theta) \tag{2}$$

$$\dot{\theta} = \omega + d_2. \tag{3}$$

Here, $q(t) = [x(t), y(t), \theta(t)]^\top \in \mathbb{R}^3$ denotes the vector of generalized coordinates, where $x(t)$ and $y(t)$ are the Cartesian coordinates of the robot in a fixed reference frame, whereas $\theta(t)$ is its orientation angle measured with respect to the x-axis. Furthermore, $t \geq 0$ stands for time, and

$$u(t) = [v(t), \omega(t)]^\top \in \mathbb{R}^2$$

is the control input vector, with $v(t) \in \mathbb{R}$ and $\omega(t) \in \mathbb{R}$ being the longitudinal and angular velocities, respectively. Notice that, from (3), the angular velocity input $\omega(t)$ represents the time derivative of the robot's orientation angle in the disturbance-free case, namely,

$\dot{\theta}(t) = \omega(t)$ when $d_2(t) = 0$. In the presence of disturbances, the angular dynamics become $\dot{\theta}(t) = \omega(t) + d_2(t)$.

The matched disturbance vector is denoted by

$$d(t) = [d_1(t), d_2(t)]^\top \in \mathbb{R}^2,$$

which accounts for additive kinematic perturbations acting on each state equation.

It is worth noting that model (1)–(3) provides a practically motivated framework for motion control analysis in the presence of exogenous perturbations. Such perturbations may represent unmodeled effects, measurement imperfections, or external influences acting on the robot's motion.

Assumption 1. *The disturbance vector $d \in \mathbb{R}^2$ is bounded and piecewise continuous. In particular, there exists a constant $D > 0$ such that*

$$\|d(t)\|_2 \leq D, \quad \forall t \geq 0, \tag{4}$$

where $\|\cdot\|_2$ denotes the Euclidean norm.

Assumption 1 is standard in the robust control literature [16,17] and ensures that the disturbance signals remain physically realizable. In particular, bounded disturbances capture the effect of modeling uncertainties, measurement imperfections, and external perturbations acting on the wheeled mobile robot.

In contrast to standard trajectory tracking approaches, the reference motion is not prescribed a priori but is generated by a dynamic auxiliary system with a stable limit cycle. Specifically, let $(x_r(t), y_r(t))$ denote the state of a reference nonlinear oscillator that will be defined in Section 3. The corresponding orientation reference $\theta_r(t)$ is defined consistently with the tangent direction of the generated motion. Thus, the reference configuration is given by $q_r(t) = [x_r(t), y_r(t), \theta_r(t)]^\top$.

Control Objective: Rather than enforcing asymptotic tracking of a predefined trajectory, the goal of this work is to asymptotically track a reference trajectory generated by dynamics possessing a stable limit cycle.

To this end, we consider the augmented system composed of the robot dynamics (1)–(3) and the reference generator. The objective is to design control inputs $v(t)$ and $\omega(t)$ such that the closed-loop trajectories converge to (or remain in a neighborhood of, in the presence of disturbances) the invariant set

$$\mathcal{O} = \left\{ (x, y, \theta, x_r, y_r) : (x, y) = (x_r, y_r),\ \theta = \theta_r,\ x_r^2 + y_r^2 = \rho^2 \right\},$$

which corresponds to the limit cycle of the reference system. The set $\mathcal{O} \subset \mathbb{R}^5$ represents the desired invariant manifold of the augmented system.

In other words, the robot is required to converge toward and evolve along the desired orbit, rather than track a specific time-parametrized trajectory.

3. Generation of Modified Van der Pol Path Reference Trajectories

This section introduces the dynamic nonlinear system used to generate the reference motion. In particular, we employ a modified Van der Pol oscillator whose limit cycle defines the desired circular orbit to be tracked by the wheeled mobile robot.

3.1. Modified Van der Pol Equation

We first recall the classical Van der Pol equation, which is a second-order scalar nonlinear differential equation, and its general representation can be given as follows:

$$\ddot{z} + \varepsilon\left[(z - z_0)^2 - \rho^2\right]\dot{z} + \mu^2(z - z_0) = 0 \tag{5}$$

with positive parameters ε, ρ, μ. Equation (5) is a special case of the Lienard equation [6]

$$\ddot{v} + r(v)\dot{v} + g(v) = 0 \tag{6}$$

where $r(v)$ and $g(v)$ are continuously differentiable functions.

The Van der Pol oscillator (5) possesses a periodic solution, known as a stable limit cycle, which serves as an attractor for all phase-space trajectories except for the unstable equilibrium point $(z, \dot{z}) = (z_0, 0)$. Specifically, since $(z_0, 0)$ is a stationary solution, a trajectory initiated exactly at this point remains there for all $t \geq 0$ and does not converge to the limit cycle. The parameter $\rho > 0$ regulates the limit cycle amplitude, $\mu > 0$ determines its frequency, $\varepsilon > 0$ influences the rate of convergence to the cycle, and the parameter z_0 is for the offset of z.

A modified version of the Van der Pol equation is proposed in [12]:

$$\ddot{z} + \varepsilon\left[z^2 + \frac{1}{\mu^2}\dot{z}^2 - \rho^2\right]\dot{z} + \mu^2 z = 0, \tag{7}$$

where, in contrast to (5), no offset term is present. Equation (7) can also be interpreted as a Liénard system (6), with

$$r(v) = \varepsilon\left[v^2 + \frac{1}{\mu^2}\dot{v}^2 - \rho^2\right], \qquad g(v) = \mu^2 v.$$

Theorem 1 ([12]). *Consider the modified Van der Pol Equation* (7) *with positive parameters* ε, μ, ρ. *Then, Equation* (7) *admits a unique stable limit cycle given by the ellipse*

$$z^2 + \frac{\dot{z}^2}{\mu^2} = \rho^2, \tag{8}$$

which attracts all trajectories except the unstable equilibrium $z = \dot{z} = 0$.

The result of Theorem 1 establishes that the modified Van der Pol system admits a unique invariant limit cycle with explicit geometric structure. This property is fundamental for the control design developed in this work, as it provides a dynamically generated orbit toward which the robot motion is driven.

The orbital stability analysis of Theorem 1 is concluded by proposing the positive definite function

$$V(z, \dot{z}) = \frac{1}{2}z^2 + \frac{1}{2\mu^2}\dot{z}^2. \tag{9}$$

The time derivative of the Lyapunov function candidate along the solution of (7) is

$$\dot{V}(z, \dot{z}) = \frac{\varepsilon}{\mu^2}\left[\rho^2 - \left(z^2 + \frac{\dot{z}^2}{\mu^2}\right)\right]\dot{z}^2. \tag{10}$$

Therefore,

$$\dot{V}(z,\dot{z}) = \begin{cases} > 0 & \text{if } \left(z^2 + \frac{\dot{z}^2}{\mu^2}\right) < \rho^2 \text{ and } \dot{z} \neq 0, \\ < 0 & \text{if } \left(z^2 + \frac{\dot{z}^2}{\mu^2}\right) > \rho^2 \text{ and } \dot{z} \neq 0, \\ = 0 & \text{if } \left[\rho^2 - \left(z^2 + \frac{\dot{z}^2}{\mu^2}\right)\right]\dot{z} = 0 \end{cases} \tag{11}$$

on the trajectories of Equation (7). By applying the invariance principle [18] to (11), one concludes that the trajectories converge to the largest invariant set contained in the set $\{(z,\dot{z}) : V(z,\dot{z}) = 0\}$, where

$$\left[\rho^2 - \left(z^2 + \frac{\dot{z}^2}{\mu^2}\right)\right]\dot{z} = 0. \tag{12}$$

Since the origin is a unique equilibrium point of (7), all the trajectories of (7) cross the axis $\dot{z} = 0$ everywhere except the origin. Hence, the largest invariant manifold of set (12) coincides with the ellipse (8), and it is straightforwardly verified that (8) is a limit cycle of the modified Van der Pol Equation (7).

3.2. Transforming the Modified Van der Pol Equation into a Path Reference Trajectory

To obtain a planar representation of the oscillator dynamics, we introduce the coordinate transformation

$$x_r(t) := z(t), \qquad y_r(t) := \frac{\dot{z}(t)}{\mu}, \tag{13}$$

where $x_r(t) \in \mathbb{R}$ and $y_r(t) \in \mathbb{R}$ denote the planar coordinates of the reference trajectory obtained from the transformed modified Van der Pol oscillator dynamics.

Under this change in variables, the resulting reference dynamics are

$$\dot{x}_r = \mu y_r, \tag{14}$$

$$\dot{y}_r = -\mu x_r - \varepsilon\left[x_r^2 + y_r^2 - \rho^2\right] y_r. \tag{15}$$

It follows directly from Theorem 1 that the trajectories of (14) and (15) converge to the invariant set

$$x_r^2 + y_r^2 = \rho^2,$$

which defines a circular limit cycle in the plane. Therefore, the system of (14) and (15) acts as a nonlinear oscillator whose dynamics generate the desired orbit.

Finally, the path–tangential orientation reference is defined as

$$\theta_r = \arctan\left(\frac{\dot{y}_r}{\dot{x}_r}\right) = \arctan\left(\frac{-\mu x_r - \varepsilon\left(x_r^2 + y_r^2 - \rho^2\right)}{\mu y_r}\right). \tag{16}$$

By construction, the reference trajectory $q_r = [x_r, y_r, \theta_r]^T$ is smooth, and its orientation $\theta_r(t)$ is aligned with the tangent to the planar motion. Moreover, due to the limit-cycle behavior of the modified Van der Pol oscillator, the resulting motion converges to a periodic orbit, which defines the target invariant set for the control design.

Figure 1 shows the trajectory of the modified Van der Pol oscillator superimposed on its vector field. This phase-plane representation not only illustrates the nonlinear dynamics governing the state evolution but also provides an intuitive visualization of how the trajectories converge to the limit cycle of the reference dynamics (14)–(16).

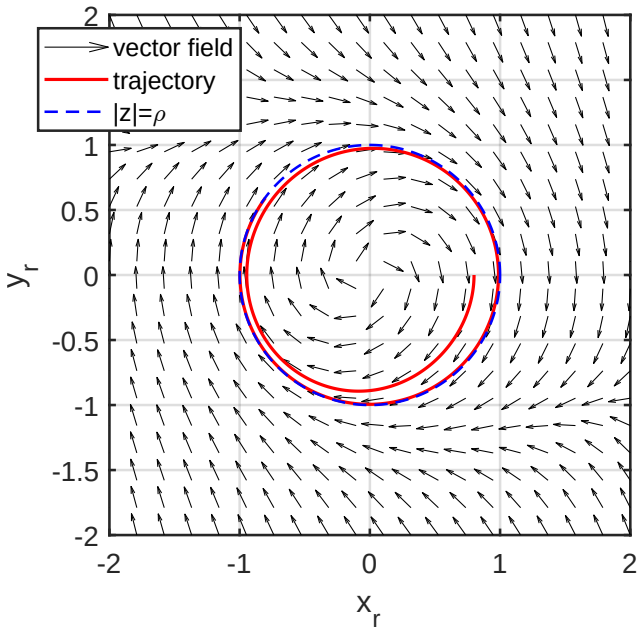

Figure 1. Phase portrait of the Van der Pol equation: the solid red curve corresponds to the reference van der Pol trajectory spiraling toward the dashed blue circle, and the dashed arrows represent the vector field on the phase plane.

Direction of circulation and traffic interpretation: The limit cycle defined by $x_r^2 + y_r^2 = \rho^2$ represents a circular path whose geometry is independent of the direction of traversal. In applications such as roundabout navigation, the direction of circulation (clockwise or counterclockwise) is dictated by traffic rules. This can be incorporated without modifying the oscillator structure.

Specifically, the direction of motion can be reversed by defining

$$\theta_r = \arctan\left(\frac{\dot{y}_r}{\dot{x}_r}\right) + \pi, \tag{17}$$

which aligns the reference orientation with the opposite tangential direction. Equivalently, reversing the vector field $(\dot{x}_r, \dot{y}_r) \to -(\dot{x}_r, \dot{y}_r)$, preserves the invariant set while changing the direction of circulation. This flexibility allows the same dynamically generated reference to accommodate both traffic conventions, while retaining the transient advantages induced by the intrinsic attractivity of the modified Van der Pol dynamics.

4. Tracking Control Design

In this section, we carry out the synthesis of a robust nonlinear control law for a perturbed wheeled robot (1)–(3).

4.1. Kinematic Reference Model

First, let us propose the following kinematic reference model:

$$\dot{q}_r = \begin{bmatrix} \cos(\theta_r) & 0 \\ \sin(\theta_r) & 0 \\ 0 & 1 \end{bmatrix} \begin{bmatrix} v_r \\ \omega_r \end{bmatrix}, \tag{18}$$

which defines the reference motion associated with the Van der Pol dynamics (14)–(16). Here, $v_r(t)$ is the desired longitudinal velocity, and $\omega_r(t)$ is the desired angular velocity.

We next define the reference linear and angular velocities $v_r(t)$ and $\omega_r(t)$ so that the reference trajectory (x_r, y_r, θ_r) is consistent with the Van der Pol dynamics (13)–(16). These

quantities are computed directly from the parametrization of the reference path. Specifically, the linear velocity is given by

$$\begin{aligned} v_r(t) &= \sqrt{\dot{x}_r^2 + \dot{y}_r^2} \\ &= \sqrt{(\mu y_r)^2 + \big(-\mu x_r - \varepsilon(x_r^2 + y_r^2 - \rho^2)y_r\big)^2}, \end{aligned} \tag{19}$$

where the relation (13) is used.

To derive an explicit expression for $\omega_r(t)$, we first note from (14) and (15) that

$$\dot{x}_r = \mu y_r,$$

and

$$\dot{y}_r = -\mu x_r - \varepsilon(x_r^2 + y_r^2 - \rho^2)y_r.$$

Differentiating the above expressions with respect to time yields

$$\ddot{x}_r = \mu \dot{y}_r,$$

and

$$\ddot{y}_r = -\mu \dot{x}_r - \varepsilon \frac{d}{dt}\Big((x_r^2 + y_r^2 - \rho^2)y_r\Big).$$

Introducing the notation

$$r^2 := x_r^2 + y_r^2,$$

and applying the product rule, one obtains

$$\ddot{y}_r = -\mu \dot{x}_r - \varepsilon\Big(2x_r\dot{x}_r y_r + 2y_r^2\dot{y}_r + (r^2 - \rho^2)\dot{y}_r\Big).$$

Substituting $\dot{x}_r$, $\dot{y}_r$, $\ddot{x}_r$, and $\ddot{y}_r$ into

$$\omega_r(t) = \frac{\dot{x}_r\ddot{y}_r - \dot{y}_r\ddot{x}_r}{\dot{x}_r^2 + \dot{y}_r^2}, \tag{20}$$

followed by straightforward algebraic simplifications, yields

$$\omega_r(t) = \frac{\mu(2\varepsilon^2(r^2 - \rho^2)y_r^4 - \mu\varepsilon x_r y_r(r^2 - \rho^2) - \mu^2 r^2)}{\mu^2 r^2 \; + \; 2\mu\varepsilon x_r y_r(r^2 - \rho^2) \; + \; \varepsilon^2(r^2 - \rho^2)^2 y_r^2}. \tag{21}$$

The resulting parametrization is used next for feedback controller design.

Regarding the well-posedness of (21), it is important to note that the proposed maneuver corresponds to a roundabout-entry problem. Consequently, the reference trajectory is initialized outside the desired limit cycle, such that

$$r(0) > \rho.$$

Since the limit cycle is an attractor for the modified Van der Pol dynamics (excluding the origin), the exterior region

$$\Omega = \Big\{(x_r, y_r) \in \mathbb{R}^2 : \; x_r^2 + y_r^2 \geq \rho^2\Big\}$$

is forward invariant. This ensures that $r(t) \geq \rho$ for all $t \geq 0$.

To establish that ω_r is free of singularities, let D denote the denominator in (21):

$$D = \mu^2 r^2 + 2\mu\varepsilon x_r y_r(r^2 - \rho^2) + \varepsilon^2(r^2 - \rho^2)^2 y_r^2.$$

By utilizing the identity $x_r^2 + y_r^2 = r^2$, this expression can be rearranged into a sum of non-negative squares:

$$D = \left[\mu r + \varepsilon(r^2 - \rho^2)\frac{x_r y_r}{r}\right]^2 + \varepsilon^2(r^2 - \rho^2)^2\frac{y_r^4}{r^2}.$$

Hence, D is a sum of non-negative terms. Moreover, for D to vanish, the second term requires either $r = \rho$ or $y_r = 0$. In both cases, the first term reduces to $\mu^2 r^2$. Since the considered trajectories satisfy $r(t) \geq \rho$, it follows that

$$D(x_r, y_r) \geq \mu^2\rho^2 > 0, \qquad \forall (x_r, y_r) \in \Omega.$$

Thus, the denominator is uniformly bounded away from zero throughout the transient and steady-state phases. This confirms that ω_r is well-defined and that the reference dynamics are well-posed under the specified initialization conditions.

4.2. Error Dynamics

For controller synthesis, the tracking errors are expressed in the robot's body-fixed coordinate frame. This choice is suitable since it reveals a cascaded structure in the closed-loop error dynamics, which is instrumental in constructing Lyapunov function candidates and subsequent stability analysis.

The tracking errors in the body-fixed frame are defined as

$$\begin{bmatrix} e_1 \\ e_2 \\ e_3 \end{bmatrix} = \begin{bmatrix} \cos(\theta) & \sin(\theta) & 0 \\ -\sin(\theta) & \cos(\theta) & 0 \\ 0 & 0 & 1 \end{bmatrix} \begin{bmatrix} x_r - x \\ y_r - y \\ \theta_r - \theta \end{bmatrix}. \tag{22}$$

Differentiating (22) along the trajectories of the robot kinematics (1)–(3) and using the reference relations $\dot{x}_r = v_r \cos\theta_r$, $\dot{y}_r = v_r \sin\theta_r$ from (18), the tracking error dynamics results in

$$\dot{e}_1 = e_2\omega + v_r\cos(e_3) - v + d_1 \tag{23}$$
$$\dot{e}_2 = -e_1\omega + v_r\sin(e_3), \tag{24}$$
$$\dot{e}_3 = \omega_r - \omega + d_2, \tag{25}$$

where $v(t) \in \mathbb{R}$ and $\omega(t) \in \mathbb{R}$ denote the control inputs to be designed.

4.3. Control Design and Stability Analysis

The proposed robust tracking controller is

$$v = k_1 e_1 + k_s\,\mathrm{sign}(e_1) + v_r\cos(e_3), \tag{26}$$
$$\omega = \omega_r + k_2 v_r e_2 + k_3\sin(e_3), \tag{27}$$

where k_1, k_2, k_3, and k_s are positive constants.

By substituting (26) and (27) into (23)–(25), the following closed-loop system is obtained:

$$\dot{e}_1 = e_2 w_r + k_2 v_r e_2^2 + k_3 e_2\sin(e_3) - k_1 e_1 - k_s\,\mathrm{sign}(e_1) + d_1 \tag{28}$$
$$\dot{e}_2 = -w_r e_1 - k_2 v_r e_1 e_2 - k_3 e_1\sin(e_3) + v_r\sin(e_3) \tag{29}$$
$$\dot{e}_3 = -k_2 v_r e_2 - k_3\sin(e_3) + d_2. \tag{30}$$

The closed-loop error dynamics are discontinuous because of the term $k_s \operatorname{sign}(e_1)$. Assuming the disturbances $d_1(t)$ and $d_2(t)$ are bounded and Lebesgue-measurable, the corresponding solutions are defined in the sense of Filippov [19].

Theorem 2. *Consider the closed-loop system obtained from* (1)–(3) *under the control law* (26) *and* (27). *Suppose that Assumption 1 holds. Then, for any initial condition such that* $|e_3(0) < \pi|$ *and* $(x_r(0), y_r(0)) \neq (z_0, 0)$*:*

1. *The closed-loop system* (28)–(30) *admits forward-complete Filippov solutions, since the right-hand side is measurable and locally bounded and satisfies a linear growth condition.*
2. *In the disturbance-free case, the tracking errors satisfy*

$$e(t) \to 0 \quad \text{as } t \to \infty.$$

3. *In the presence of bounded disturbances* $d_1, d_2 \in \mathbb{R}$ *satisfying Assumption 1 and provided that* $k_s > D$*, the tracking error system is uniformly ultimately bounded. More precisely,* e_1 *and* $\sin(e_3)$ *converge to a disturbance-dependent residual set, while the complete error vector* (e_1, e_2, e_3) *remains bounded for all* $t \geq 0$.

Consequently, in the disturbance-free case, the robot trajectory $(x(t), y(t))$ *asymptotically converges to the invariant set*

$$\mathcal{C} = \{(x, y) \in \mathbb{R}^2 : x^2 + y^2 = \rho^2\},$$

which corresponds to the limit cycle of the reference dynamics. Under bounded disturbances, the robot trajectory remains ultimately bounded in a neighborhood of this invariant set, with a bound depending on D.

Proof. To conclude stability, let us consider the following Lyapunov function:

$$V = \frac{1}{2}e_1^2 + \frac{1}{2}e_2^2 + \frac{1}{k_2}(1 - \cos(e_3)). \tag{31}$$

The time derivative of V along the trajectories of the closed-loop system is

$$\begin{aligned}
\dot{V} &= e_1\dot{e}_1 + e_2\dot{e}_2 + \frac{1}{k_2}\sin(e_3)\dot{e}_3 \\
&= e_1\left[e_2\omega_r + k_2 v_r e_2^2 + k_3 e_2 \sin(e_3) - k_1 e_1 - k_s \operatorname{sign}(e_1)\right] \\
&\quad + e_2[-\omega_r e_1 - k_2 v_r e_1 e_2 - k_3 \sin(e_3) e_1 + v_r \sin(e_3)] \\
&\quad + \frac{1}{k_2}\sin(e_3)[-k_2 v_r e_2 - k_3 \sin(e_3)] \\
&\quad + e_1 d_1 + \frac{1}{k_2}\sin(e_3) d_2 \\
&= -k_s|e_1| - k_1 e_1^2 - \frac{k_3}{k_2}\sin^2(e_3) + e_1 d_1 + \frac{1}{k_2}\sin(e_3) d_2.
\end{aligned} \tag{32}$$

In the disturbance-free case, that is, for $d_1 = d_2 = 0$, one has

$$\dot{V} = -k_s|e_1| - k_1 e_1^2 - \frac{k_3}{k_2}\sin^2(e_3) \leq 0.$$

From the invariance principle for differential inclusions [15], every solution converges to the largest invariant set contained in

$$\{(e_1, e_2, e_3) : \dot{V} = 0\} = \{(e_1, e_2, e_3) : e_1 = 0,\ \sin(e_3) = 0\}.$$

Within this set, we have $e_1 \equiv 0$ and $\sin(e_3(t)) \equiv 0$ for all $t \geq 0$. The condition $\sin(e_3(t)) \equiv 0$ implies that its time derivative must also vanish, i.e., $\dot{e}_3 \equiv 0$. Substituting these identities into the error dynamics (30), we have $0 = -k_2 v_r(t) e_2$. Provided that $v_r(t) \neq 0$ for all $t \geq 0$ (or is persistently exciting), it follows that $e_2 \equiv 0$. Thus, the largest invariant set is reduced to the origin

$$\mathcal{S} = \{(e_1, e_2, e_3) : e_1 = 0,\ e_2 = 0,\ \sin(e_3) = 0\},$$

establishing the asymptotic stability of the tracking error.

Since the reference dynamics satisfy

$$x_r^2 + y_r^2 \to \rho^2,$$

and the tracking errors satisfy $e_1, e_2 \to 0$, it follows that

$$[x(t), y(t)] \to [x_r(t), y_r(t)].$$

Therefore, the robot trajectory asymptotically converges to the invariant limit cycle induced by the reference dynamics. Under the condition $|e_3(0)| < \pi$, the solution converges to the equilibrium $e_3 = 0$.

For the perturbed case, from Assumption 1 and from the definition of the Euclidean norm, it follows that

$$|d_1(t)| \leq D, \qquad |d_2(t)| \leq D, \qquad \forall t \geq 0.$$

Therefore,

$$\begin{aligned} \dot{V} &\leq -k_s|e_1| - k_1 e_1^2 - \frac{k_3}{k_2}\sin^2(e_3) + D|e_1| + \frac{D}{k_2}|\sin(e_3)| \\ &= -(k_s - D)|e_1| - k_1 e_1^2 - \frac{k_3}{k_2}\sin^2(e_3) + \frac{D}{k_2}|\sin(e_3)|. \end{aligned} \tag{33}$$

Using Young's inequality,

$$\frac{D}{k_2}|\sin(e_3)| \leq \frac{k_3}{2k_2}\sin^2(e_3) + \frac{D^2}{2k_2k_3},$$

Therefore, provided that $k_s > D$, the Lyapunov function is nonincreasing outside a disturbance-dependent residual set characterized by

$$\dot{V} \leq -(k_s - D)|e_1| - k_1 e_1^2 - \frac{k_3}{2k_2}\sin^2(e_3) + \frac{D^2}{2k_2k_3}. \tag{34}$$

Consequently, e_1 and $\sin(e_3)$ are uniformly ultimately bounded, with an ultimate bound depending explicitly on the disturbance magnitude D. Since V is positive definite in e_1, e_2, and $1 - \cos(e_3)$, the boundedness of V also guarantees boundedness of the complete error vector (e_1, e_2, e_3), modulo the angular periodicity of e_3. □

5. Simulation Results

The simulated navigation of the wheeled mobile robot was carried out in Matlab/Simulink 2024b to evaluate the tracking performance with respect to the modified Van der Pol limit-cycle reference trajectory (14) and (15).

Figure 2 shows the robot trajectory tracking the reference limit cycle, together with the corresponding tracking errors of the closed-loop system in the disturbance-free case.

The controller gains in (26) and (27) were set to $k_1 = 0.8$, $k_2 = 2.0$, $k_3 = 12.5$, and $k_s = 2.5$, whereas the parameters of the reference model (14)–(16) were $\mu = 1.0$, $\varepsilon = 0.8$, and $\rho = 2.0$.

The robot is initialized at $x(0) = -3.1$, $y(0) = 0.27$, and $\theta(0) = \pi/4$, while the reference trajectory starts from $x_r(0) = -3$, $y_r(0) = 0.25$, and $\theta_r(0) = \pi/4$. These initial conditions were chosen to be close but not identical and were intentionally set outside the limit cycle, reflecting the realistic scenario of a vehicle approaching and entering a roundabout.

The results show that the robot converges smoothly to the desired orbit without exhibiting noticeable oscillatory transients or overshoot. The tracking errors (e_1, e_2, e_3), shown in Figure 2c, converge to zero, confirming the effectiveness of the proposed control law. In particular, the position errors (e_1, e_2) decrease, while the orientation error e_3 also converges to zero. Figure 2d,e show the orientation and angular velocities of the wheeled mobile robot, respectively. These results show that the proposed control strategy ensures asymptotic trajectory tracking and convergence to the desired limit cycle under nominal conditions.

Figure 3 illustrates the robot trajectory tracking the reference limit cycle, together with the corresponding tracking errors of the closed-loop system under perturbed conditions. The applied matched disturbances are given by $d_1(t) = 0.25\sin(0.5t)$ and $d_2(t) = 0.15\cos(0.7t)$. Figure 3a depicts the robot trajectory and the reference limit cycle in the (x, y)-plane. Despite the presence of disturbances, the robot still converges toward to the desired periodic orbit with a smooth transient response. Figure 3b shows the time evolution of the tracking errors (e_1, e_2, e_3). It can be observed that all errors remain bounded and converge to a small neighborhood of the origin. Finally, Figure 3d,e show the orientation and angular velocities of the wheeled mobile robot, respectively. In particular, the position errors (e_1, e_2) exhibit damped transient responses, while the orientation error e_3 rapidly decreases and remains close to zero.

These results indicate that the proposed control law preserves satisfactory tracking performance in the presence of bounded matched disturbances, ensuring practical convergence to the desired limit cycle.

Finally, Figure 4 shows the robot trajectory tracking a circular geometric reference trajectory, together with the corresponding tracking errors of the closed-loop system in the unperturbed case. Although the robot initial condition is the same, the closed-loop system exhibits a larger transient overshoot due to the larger initial tracking error compared to the modified Van der Pol-based reference trajectory. In Figure 2, the peak values of v and ω are 4 m/s and 6 rad/s, respectively, whereas for circular trajectory tracking, they are 4 m/s and 12 rad/s. This reflects a more abrupt transient and less smooth convergence toward the desired orbit.

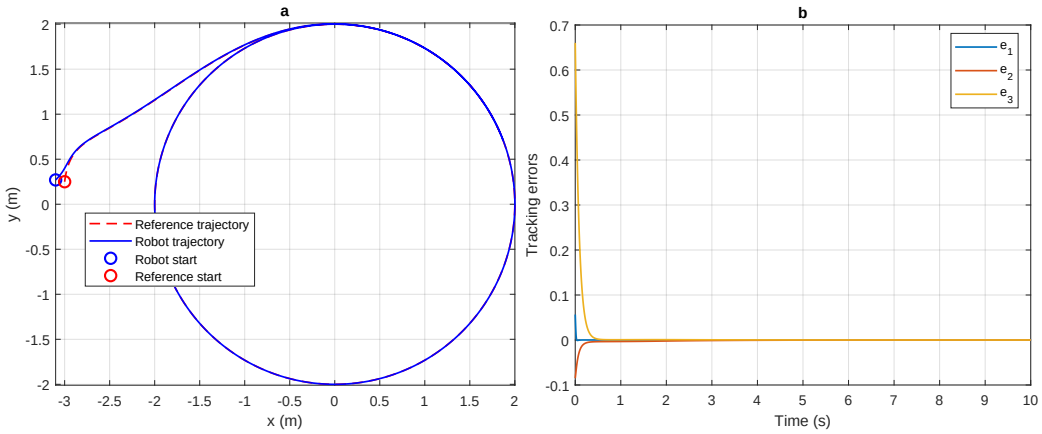

Figure 2. *Cont.*

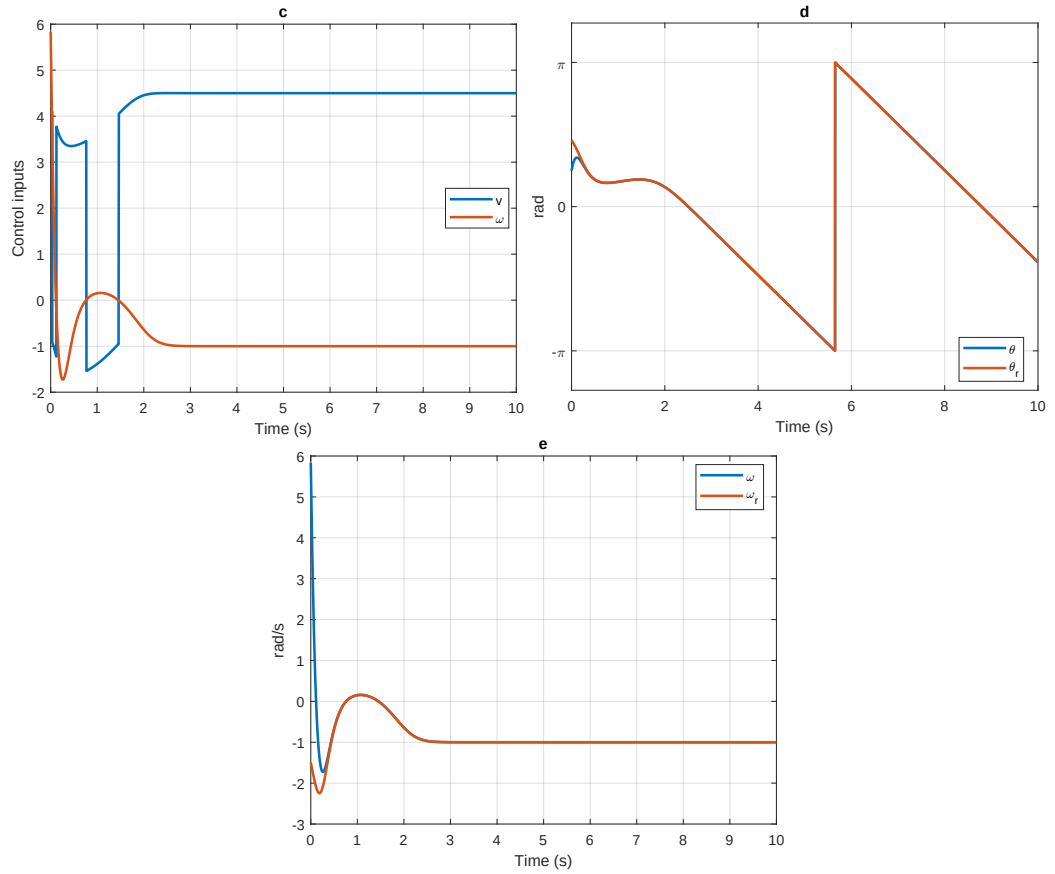

Figure 2. (**a**) Robot trajectory tracking the modified Van der Pol limit-cycle reference, (**b**) corresponding closed-loop tracking errors, (**c**) control inputs, (**d**) orientation angles, and (**e**) angular velocities under the disturbance-free case.

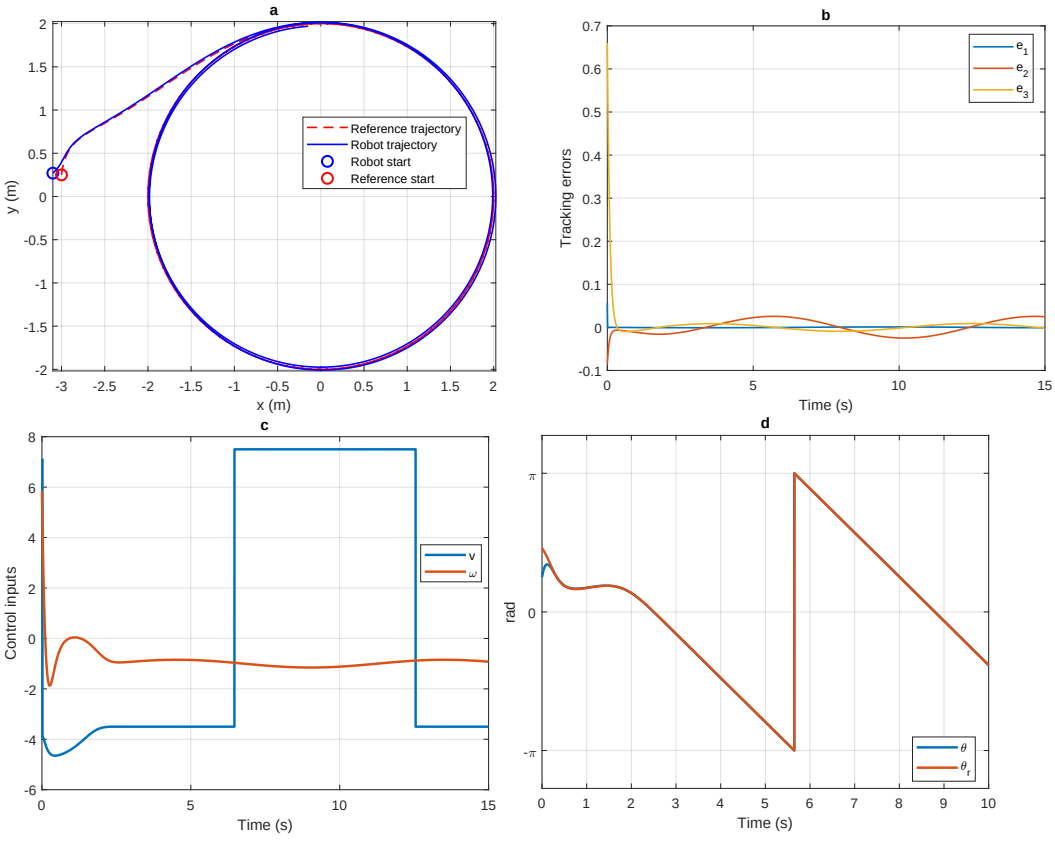

Figure 3. *Cont*.

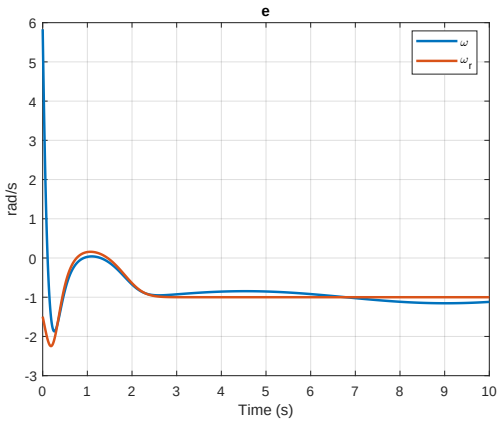

Figure 3. (**a**) Robot trajectory tracking the modified Van der Pol limit-cycle reference, (**b**) corresponding closed-loop tracking errors, (**c**) control inputs, (**d**) orientation angles, and (**e**) angular velocities for the perturbed case.

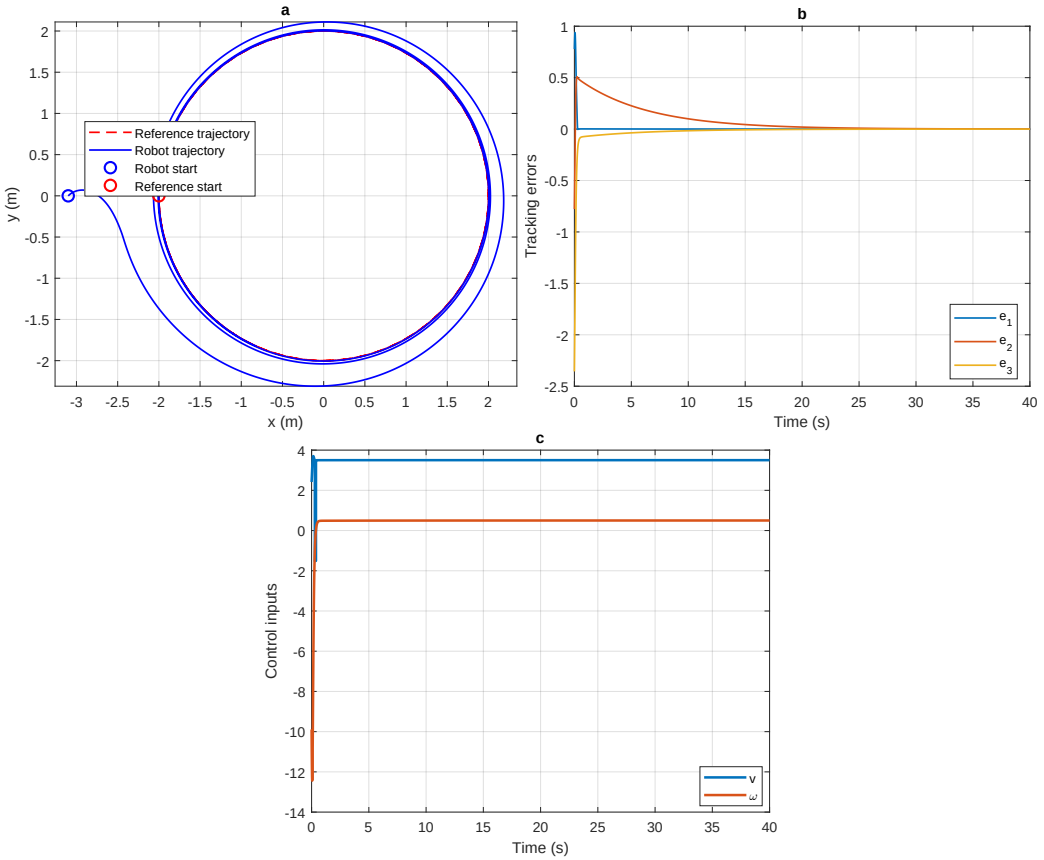

Figure 4. (**a**) Robot trajectory tracking of a circular reference trajectory, (**b**) corresponding tracking errors of the closed-loop system for the unperturbed case, and (**c**) control inputs.

6. Experimental Results

The tracking performance was experimentally evaluated using a differential-drive mobile robot with respect to two reference trajectories: a modified Van der Pol limit cycle and a geometric circle. The experimental platform, denoted as Qrobot (see Figure 5), is a custom-built system for autonomous navigation. It consists of a rectangular chassis with length $L_c = 23$ cm, width $W = 12$ cm, and height $H = 15$ cm. The differential-drive configuration has a wheelbase of $L_b = 20$ cm and a wheel radius of $R_w = 6.6$ cm.

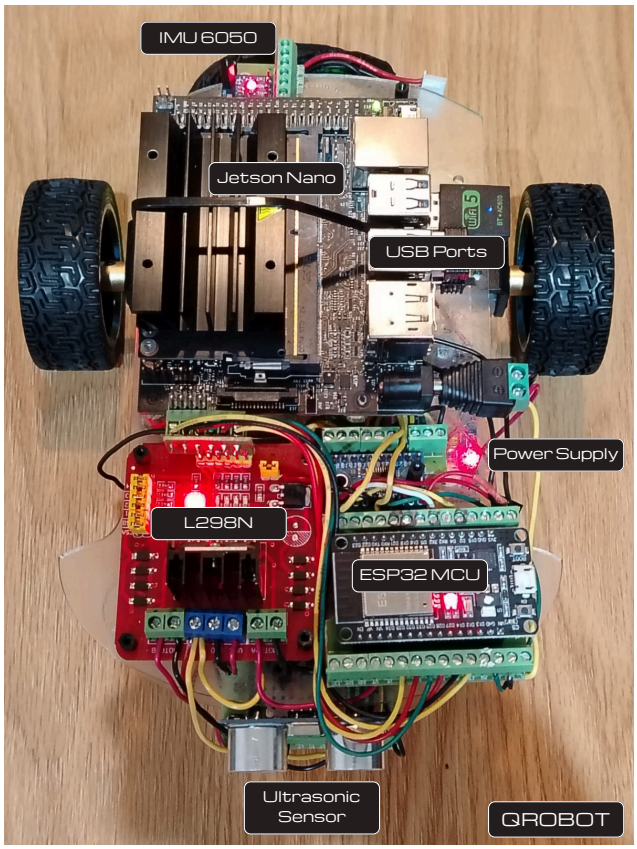

Figure 5. Mobile robot used for the experiments.

The system architecture adopted a dual-processing scheme. High-level computation was performed on an NVIDIA Jetson Nano (NVIDIA Corporation, Santa Clara, CA, USA), where the reference trajectory was generated via the modified Van der Pol dynamics, and the control law was evaluated. Low-level actuation and real-time sensor acquisition were handled by an ESP32 microcontroller (Shenzhen DOIT, Shenzhen, China). The states of the robot were estimated using wheel encoder measurements combined with an onboard inertial measurement unit IMU MPU-6050 (TDK Corporation, Tokyo, Japan), providing the feedback required for closed-loop control. The control algorithms were implemented in Python 3.6.9 within a Linux-based environment (Ubuntu 18.04.6 LTS) on the Jetson platform.

In the experimental implementation, the discontinuous term $k_s \,\mathrm{sign}(e_1)$ was directly implemented without introducing a smooth approximation. Since chattering cannot be completely eliminated in practice, the gain k_s was selected empirically to avoid excitation of resonant frequencies within the actuator bandwidth (see, e.g., [20,21]). Moreover, due to finite sampling, actuator dead-zone effects, and unmodeled dynamics, the closed-loop system exhibited practical convergence toward the desired orbit, characterized by small residual oscillations around the limit cycle.

Figure 6a shows the experimental trajectory of the robot tracking the limit cycle reference, together with the corresponding closed-loop tracking errors shown in Figure 6b and the corresponding control inputs in Figure 6c. The controller gains in (26) and (27) were set to $k_1 = 2.5$, $k_2 = 35.0$, $k_3 = 2.5$, and $k_s = 0.015$, while the parameters of the reference model (14)–(16) were $\mu = 1.0$, $\varepsilon = 2.0$, and $\rho = 0.69$. The robot was initialized at $x(0) = -0.85$ m, $y(0) = -0.2$ m, and $\theta(0) = \pi/2$ rad, all expressed with respect to the origin of the inertial frame, while the reference trajectory was initialized from a nearby but distinct initial condition.

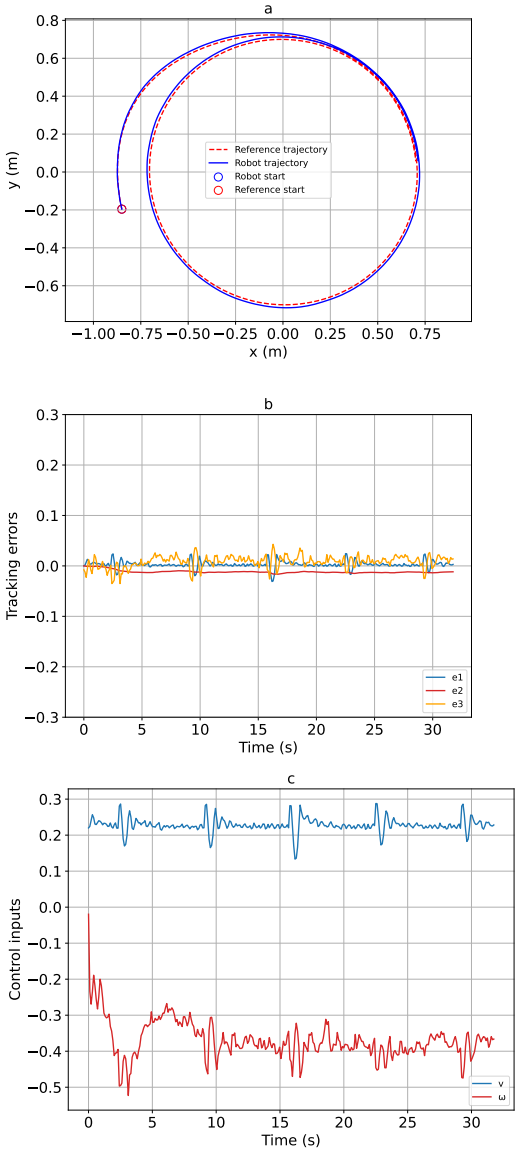

Figure 6. (**a**) Experimental robot trajectory tracking the modified Van der Pol limit-cycle reference, (**b**) corresponding closed-loop tracking errors, and (**c**) control inputs.

The tracking errors $[e_1, e_2, e_3]^\top$ remained bounded throughout the experiment; in particular, the position errors $e_1(t)$ and $e_2(t)$ were confined within approximately ± 0.04 m. The corresponding control inputs exhibited moderate amplitudes, with peak values of v and ω of approximately 0.3 m/s and -0.55 rad/s, respectively, indicating accurate tracking with low control effort.

Figure 7a illustrates the robot trajectory tracking a geometric circular reference of radius 0.69 m, with the corresponding tracking errors of the closed-loop system in Figure 7b and the control inputs in Figure 7c. Although the WMR was initialized identically to the previous experiment, the resulting tracking error peaks in the two scenarios clearly highlight the advantage of the proposed dynamic approach. For the circular geometric reference, the system exhibited a pronounced initial transient, with tracking error peaks of approximately $e_1 = 0.24$ m, $e_2 = -0.16$ m, and $e_3 = 0.31$ rad, followed by convergence to a steady state after approximately 5 s. In contrast, under the modified Van der Pol reference, the position errors e_1 and e_2 avoided large initial deviations, remaining tightly bounded within approximately ± 0.04 m throughout the experiment.

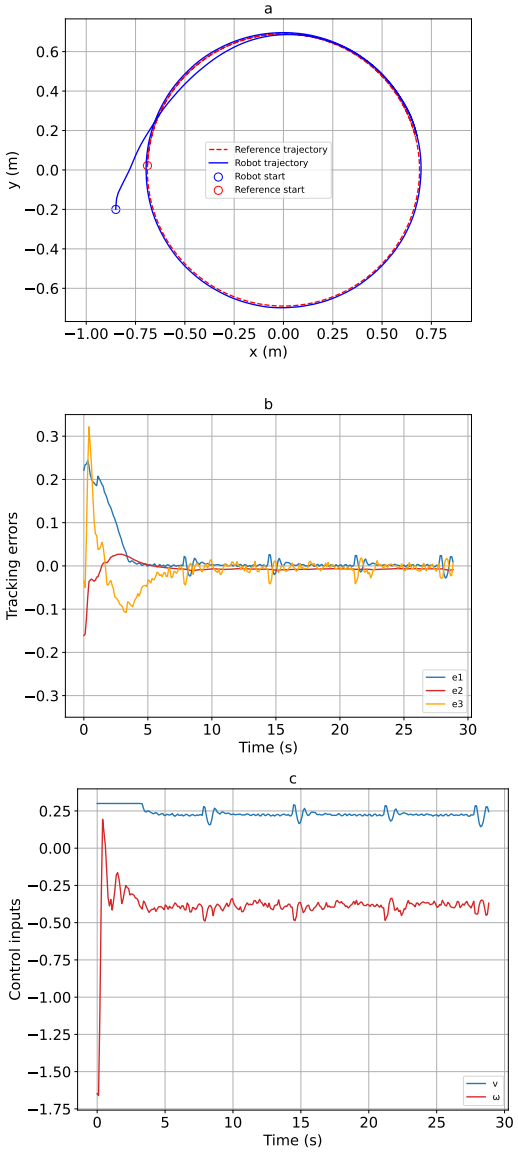

Figure 7. (**a**) Experimental robot trajectory tracking the geometric circular reference, (**b**) corresponding closed-loop tracking errors, and (**c**) control inputs.

Consistent with the simulation results, this clear contrast in error peaks indicates that the geometric reference induces significantly larger initial tracking errors when the robot is initialized away from the path. In contrast, the modified Van der Pol formulation yields improved transient behavior by providing a dynamically evolving reference, which guides the robot toward the desired limit cycle, thereby avoiding large initial deviations and abrupt control actions associated with predefined geometric paths.

To quantitatively substantiate the advantage introduced by the transient deformation, an additional numerical comparison of the absolute position and orientation tracking errors during the first 5 s of the transient phase was conducted, as shown in Figure 8. The results indicate that the geometric circular reference generates significantly larger transient errors due to the initial mismatch between the robot state and the prescribed orbit, namely, $\|e(0)_{\mathrm{VDP}}\| < \|e(0)_{\mathrm{circle}}\|$. In particular, the circular reference produces a peak position error of approximately 0.40 m, whereas the modified VDP reference confines the error to only 0.04 m. Likewise, the absolute orientation error $|e_3|$ associated with the circular reference exhibits a pronounced transient peak of 0.31 rad, while the VDP-based reference maintains a smooth evolution that remains below 0.05 rad. These quantitative error metrics

confirm that the dynamically generated reference trajectory substantially mitigates the severe transient tracking errors typically induced by static geometric references.

It is important to note that the stability analysis in Equations (1)–(3) assumes matched disturbances. In practical WMR applications, factors such as nonholonomic slip and actuator dynamics introduce unmatched uncertainties that do not enter the system through the control input channel. While a formal stability proof for unmatched disturbances often requires more complex techniques (such as higher-order SMC or integral SMC), the standard SMC employed here provides a high degree of practical robustness. By selecting sufficiently high control gains, the system state is maintained within a boundary layer of the sliding surface. The experimental results presented in this section confirm that the proposed framework remains robust under these nonideal conditions, effectively compensating for the physical limitations of the robot platform.

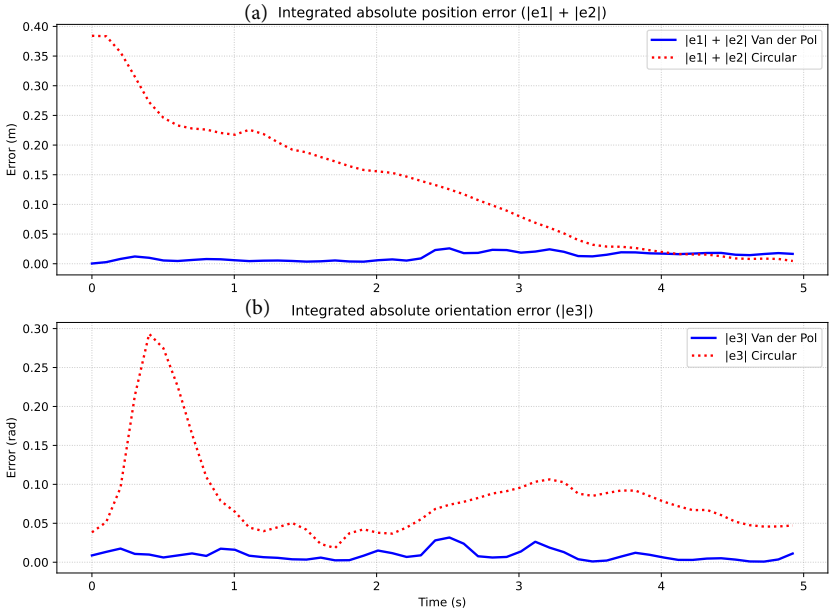

Figure 8. Quantitative comparison of separated absolute tracking errors during the 5 s transient phase: (**a**) sum of absolute position errors $|e_1| + |e_2|$ in meters; (**b**) absolute orientation error $|e_3|$ in radians.

7. Conclusions

In this paper, a control framework for wheeled mobile robots based on a dynamically generated reference trajectory was proposed. The desired motion is defined by a modified Van der Pol oscillator, whose limit cycle provides an invariant set corresponding to a circular orbit. In contrast to standard approaches based on predefined geometric paths, the proposed formulation enables smooth convergence toward the desired orbit from a wide set of initial conditions.

A robust control law was designed for a perturbed nonholonomic robot model, and the resulting closed-loop system was analyzed within the framework of Lyapunov functions for discontinuous systems. It was shown that the tracking errors converge asymptotically to zero in the disturbance-free case, while, under bounded matched disturbances, the closed-loop trajectories remain uniformly ultimately bounded. As a consequence, the robot trajectory converges to the limit cycle of the reference dynamics, thereby ensuring asymptotic tracking of the dynamically generated limit-cycle motion.

The proposed approach provides a systematic way to embed desired periodic behaviors into the control design via dynamic nonlinear systems, offering improved transient performance compared to static path-following methods.

Future research will investigate hybrid control strategies enabling safe transitions from the stabilized limit cycle to exit trajectories. In addition, extensions to multi-lane scenarios through adaptive modulation of the oscillator parameters will be considered. The incorporation of dynamic obstacle avoidance and learning-based components also represents a promising direction for enhancing performance in complex and uncertain environments.

Author Contributions: Conceptualization, J.Q., L.T.A., U.O.-R. and V.M.J.-L.; methodology, J.Q.; software, J.Q.; validation, J.Q.; resources, J.Q., L.T.A. and U.O.-R.; writing—original draft preparation, J.Q. and L.T.A.; writing—review and editing, L.T.A., U.O.-R. and V.M.J.-L.; supervision, L.T.A. and U.O.-R. All authors have read and agreed to the published version of the manuscript.

Funding: This work was partially supported by Instituto Politecnico Nacional under grants SIP IND-2026-0008 and SIP 2026-0065 and by TecNM under grant 26471.26-P. V. Juárez-Luna also thanks Instituto Politécnico Nacional for the invaluable support during his sabbatical stay.

Data Availability Statement: The data presented in this study are available on request from the corresponding author.

Conflicts of Interest: The authors declare no conflicts of interest.

References

1. Li, N.; Jin, G.; Zhang, P.; Ma, W.; Tian, Y.; Lu, S.; Cao, G. Taxi Traffic Flow Prediction Based on Spatiotemporal-Fusion Graph Neural Networks. *Electronics* **2026**, *15*, 1621. [CrossRef]
2. Niu, Y.; Chang, Y.; Li, H.; Feng, X.; Ren, Y. Autonomous-Vehicle Intersection Control Method Based on an Interlocking Block. *Electronics* **2024**, *13*, 110. [CrossRef]
3. An, L.; Huang, X.; Yang, P.; Liu, Z. Adaptive bézier curve-based path following control for autonomous driving robots. *Robot. Auton. Syst.* **2025**, *189*, 104969. [CrossRef]
4. Li, B.; Shao, Z. Simultaneous dynamic optimization: A trajectory planning method for nonholonomic car-like robots. *Adv. Eng. Softw.* **2015**, *87*, 30–42. [CrossRef]
5. Van der Pol, B. Forced oscillations in a circuit with nonlinear resistance. *Philos. Mag. Ser.* **1927**, *3*, 65–80. [CrossRef]
6. Lienard, A. Étude des oscillations entretenues. *Rev. Générale l'Electricité* **1928**, *23*, 901–902.
7. Jasni, F.; Shafie, A. Van Der Pol Central Pattern Generator (VDP-CPG) Model for Quadruped Robot. In *Proceedings of the Trends in Intelligent Robotics, Automation, and Manufacturing*; Ponnambalam, S.G., Parkkinen, J., Ramanathan, K.C., Eds.; Springer: Berlin/Heidelberg, Germany, 2012; pp. 167–175.
8. Song, Z.; Wang, H.; Xu, J. A novel theoretical approach for hexapodal gait generation of the CPG controller by using the delay-coupled VDP oscillators. *IEEE Trans. Ind. Electron.* **2025**, *72*, 13606–13616. [CrossRef]
9. Kobayashi, J. Large force generation and control method of manipulator exploiting its oscillatory motion using Van Der Pol oscillator. *Int. J. Control Autom. Syst.* **2010**, *8*, 1048–1060. [CrossRef]
10. Belousov, R.; Berger, F.; Hudspeth, A. Volterra-series approach to stochastic nonlinear dynamics: Linear response of the Van der Pol oscillator driven by white noise. *Phys. Rev. E* **2020**, *102*, 032209. [CrossRef] [PubMed]
11. Okada, S.; Matsuhashi, Y.; Uchida, K. Synthesis of autonomous periodic motion of a small blimp system using the van der Pol Equation. In Proceedings of the 7th Asian Control Conference, Hong Kong, China, 27–29 August 2009; pp. 953–958.
12. Orlov, Y.; Aguilar, L.; Acho, L.; Ortiz, A. Asymptotic harmonic generator and its application to finite time orbital stabilization of a friction pendulum with experimental verification. *Int. J. Control* **2008**, *82*, 227–237. [CrossRef]
13. Orlov, Y.; Aguilar, L.; Acho, L.; Ortiz, A. Robust orbital stabilization of pendubot: Algorithm synthesis, experimental verification, and application to swing up and balancing control. In *Modern Sliding Mode Control Theory*; Springer: Berlin/Heidelberg, Germany, 2008; pp. 383–400.
14. Aguilar, L.; Orlov, Y. Limit cycle generation in Van der Pol Flavored PDE setting. *IEEE Control Syst. Lett.* **2023**, *7*, 3603–3608. [CrossRef]
15. Alvarez, J.; Orlov, Y.; Acho, L. An invariance principle for discontinuous dynamic systems with application to a Coulomb friction oscillator. *J. Dyn. Syst. Meas. Control* **2000**, *122*, 687–690. [CrossRef]
16. Orlov, Y. *Discontinuous Systems: Lyapunov Analysis and Robust Synthesis Under Uncertainty Conditions*; Springer: London, UK, 2008.
17. Shtessel, Y.; Edwards, C.; Fridman, L.; Levant, A. *Sliding Mode Control and Observation*; Birkhäuser: New York, NY, USA, 2014.
18. Khalil, H. *Nonlinear Systems*; Prentice Hall: Upper Saddle River, NJ, USA, 2002.
19. Filippov, A. *Differential Equations with Discontinuous Righthand Sides*; Kluwer Academic Publisher: Dordrecht, The Netherlands, 1988.

20. Boiko, I. *Discontinuous Control Systems: Frequency-Domain Analysis and Design*; Birkäuser: London, UK, 2009.
21. Wang, B.; Brogliato, B.; Acary, V.; Boubakir, A.; Plestan, F. Experimental Comparisons Between Implicit and Explicit Implementations of Discrete-Time Sliding Mode Controllers: Toward Input and Output Chattering Suppression. *IEEE Trans. Control Syst. Technol.* **2015**, *23*, 2071–2075. [CrossRef]